J Gastroenterol
DOI 10.1007/s00535-013-0835-9

ORIGINAL ARTICLE—LIVER, PANCREAS, AND BILIARY TRACT

Autophagy enhances hepatocellular carcinoma progression by activation of mitochondrial β-oxidation

Takeo Toshima · Ken Shirabe · Yoshihiro Matsumoto · Shohei Yoshiya · Toru Ikegami · Tomoharu Yoshizumi · Yuji Soejima · Tetsuo Ikeda · Yoshihiko Maehara

Received: 10 October 2012 / Accepted: 9 May 2013

Abstract
Background Several types of cancers, including hepatocellular carcinoma (HCC), show resistance to hypoxia and nutrient starvation. Autophagy is a means of providing macromolecules for energy generation under such stressed-conditions. The aim of this study was to clarify the role of autophagy in HCC development under hypoxic conditions.
Methods The expression of microtubule-associated protein 1 light chain 3 (LC3), which is a key gene involved in autophagosome formation, was evaluated in human HCC using immunohistochemistry and western blot. The relationship between LC3 and hypoxia-induced factor 1α (HIF1α) expression was examined using real-time PCR. In addition, human HCC cell line Huh7 was treated with pharmacological autophagy-inhibitor and inactive mutant of Atg4B ($Atg4B^{C74A}$) under hypoxic condition to evaluate the effects of hypoxia-induced autophagy on cell survival, intracellular ATP, and mitochondrial β-oxidation.
Results LC3 was significantly highly expressed in HCC as compared with noncancerous tissues. LC3 expression, correlated with HIF1α expression, was also significantly correlated with tumor size, and only in the context of large tumors, was an independent predictor of HCC recurrence after surgery. In addition, Huh7 treated with autophagy-inhibitor under hypoxia had lower viability, with low levels of intracellular ATP due to impaired mitochondrial β-oxidation.
Conclusions Autophagy in HCC works to promote HIF1α-mediated proliferation through the maintenance of intracellular ATP, depending on the activation of mitochondrial β-oxidation. These findings demonstrated the feasibility of anti-autophagic treatment as a potential curative therapy for HCC, and improved understanding of the factors determining adaptive metabolic responses to hypoxic conditions.

Keywords Autophagy · Cancer progression · Hepatocellular carcinoma

Abbreviations

AFP	Alpha-fetoprotein
Atg	Autophagy-related genes
ATP	Adenosine 5′-triphosphate
DCP	Des-gamma-carboxy prothrombin
HCC	Hepatocellular carcinoma
HIF1α	Hypoxia-induced factor 1α
ICG R15	Indocyanine green retention test at 15 min
LC3	Microtubule-associated protein 1 light chain 3
PBS	Phosphate-buffered saline
PCR	Polymerase chain reaction
PI3K	Phosphatidylinositol 3-kinase
ROS	Reactive oxygen species
SD	Standard deviation
3MA	3-Methyladenine

Introduction

Hepatocellular carcinoma (HCC) is common and increasing in incidence worldwide [1–4]. HCC grows to a

Electronic supplementary material The online version of this article (doi:10.1007/s00535-013-0835-9) contains supplementary material, which is available to authorized users.

T. Toshima · K. Shirabe (✉) · Y. Matsumoto · S. Yoshiya · T. Ikegami · T. Yoshizumi · Y. Soejima · T. Ikeda · Y. Maehara
Department of Surgery and Science, Graduate School of Medical Sciences, Kyushu University, 3-1-1 Maidashi, Higashi-ku, Fukuoka 812-8582, Japan
e-mail: kshirabe@surg2.med.kyushu-u.ac.jp

Published online: 24 May 2013

relatively large size, sometimes over 10 cm in diameter even when necrosis was observed [5] and it can easily reoccur after therapy [6]. Proliferating cancer cells in tumors growing to a large size require a good supply of nutrients and oxygen. Angiogenesis around tumors is one way of increasing blood flow to provide the required oxygen and energy to the growing tumor [7]. However, recent studies have revealed that nutrition levels, oxygen and glucose are frequently reduced in locally advanced tumors despite tumor vessels having been established [8, 9]. This suggests that the microvasculature around the tumor is structurally and functionally abnormal and not capable of supplying the blood flow needed for cancer cell growth. Furthermore, some aggressive malignant tumors, such as poorly differentiated HCC and pancreatic cancers, are clinically hypovascular [10]. Under these conditions, cancer cells are likely to encounter limited nutrients and oxygen. However, they can exhibit resistance to nutrient deprivation and continue to grow. The mechanisms by which cancer cells obtain energy sources when their external nutrient supply is limited remain is unclear.

Autophagy is a homeostatic mechanism that regulates the turnover of long-lived or damaged proteins and organelles, buffers intracellular constituents and supplies amino acids taken from degradation products of the autolysosome [11]. For the first step, the isolation membrane, a lipid bilayer structure, is developed and sequesters cytoplasmic materials such as organelles, to form autophagosomes. During this step, microtubule-associated protein 1 light chain 3 (LC3), one of the mammalian homologues of yeast autophagy-related gene (Atg) 8, is processed and activated by a ubiquitination-like reaction regulated by Atg7 and Atg3 [12]. First, LC3 proform is cleaved into a soluble form known as LC3-I, which is further modified into a membrane-bound form, LC3-II, and this is followed by recruitment into the autophagosomes. Thus, LC3 is a specific marker of autophagosome formation. Autophagosomes engulf organelles and then fuse with lysosomes to become mature autolysosomes. Accordingly, sequestrated materials are digested into amino acids in the autolysosomes by the lysosomal enzymes [13, 14].

To study the role of autophagy in HCC under hypoxia-induced metabolic stress, we examined LC3 expression as the main marker of autophagosomes, and the other corresponding autophagic genes, Atg5 and Beclin-1, in human tissue samples and HCC cell lines under hypoxic conditions. Our results suggest that high expression of autophagy has the potential to cause malignant tumors to grow in size under hypoxic condition and also promotes poor survival, which can be independently predicted by the autophagic gene LC3 in HCC.

Materials and methods

Human tissue samples

Samples from 102 patients who had undergone liver resection for HCC without preoperative treatment at the Department of Surgery and Science at the Kyushu University Hospital between January 1986 and December 2002 were analyzed using immunohistochemistry [15]. Samples from another 131 patients between January 2004 and March 2009 were analyzed by real-time polymerase chain reaction (PCR). There were no significant differences between the characteristics of HCC patients using immunohistochemistry analysis or real-time PCR analysis (Table S1). Details in Doc. S1.

Reagents and plasmid

3-Methyladenine (3MA) and an inactive mutant of Atg4B ($Atg4B^{C74A}$) were prepared as described previously [15, 16]. Details in Doc. S1.

Immunohistochemistry and immunofluorescence

Immunohistochemical staining and immunofluorescence analysis was performed as previously described [17–20]. Immunoreactivity of cytoplasmic staining in the cancerous region was independently divided into two groups, positive and negative, by two liver pathologists. Positive staining was classified if even a small area of tissue was stained. Details in Doc. S1.

Protein extraction and western blot analysis

Protein extraction and western blot analysis were performed as previously described [21]. Details in Doc. S1.

Real-time PCR

Extraction of total RNA and real-time PCR was performed as previously described [22]. Primers used for real-time PCR are shown in Table S2 and details described in Doc. S1.

Electron microscopy

Analysis of electron microscopy was performed as previously described [20, 23, 24]. For quantification of autophagosome using electron micrographs, high-powered micrographs (×8000–10000) of 10 single cells from multiple distinct low-powered fields were obtained from each specimen [23]. Details in Doc. S1.

Cell culture under hypoxic conditions

For hypoxia treatments, human HCC cell lines were incubated in a humidified hypoxic workstation (MCO-5M, Sanyo, Osaka, Japan) with final oxygen concentrations of 0.1 % O_2 using a Clark-type polarographic electrode (Animas, Frazer, PA, USA). To defect autophagosome formation, cultured cells were treated with autophagy-inhibitor using two methods, 3MA and $Atg4B^{C74A}$, and pre-incubated for 24 h followed by incubation under hypoxia. Details in Doc. S1.

Quantification of intracellular ATP

Total cellular ATP concentration was quantitated using an ATP Detection Reagent kit (Toyo-ink, Tokyo, Japan) as previously described [25]. Details in Doc. S1.

Cytofluorimetric analysis of $\Delta\Psi_m$ and mitochondrial structure

Cytofluorimetric analysis of $\Delta\Psi_m$ and alteration of mitochondrial structure during hypoxia was performed as previously described [26, 27]. Details in Doc. S1.

Measurement of β-hydroxybutyrate

β-hydroxybutyrate concentration was spectrophotometrically assayed as previously described [28]. Details in Doc. S1.

Statistical analysis

All statistical analyses were performed using JMP statistical software version 7.01 (SAS Institute Inc., Cary, NC, USA). All experiments were independently performed three times in triplicate. All variables are expressed as the mean ± standard deviation (SD). Details in Doc. S1.

Results

Upregulation of LC3 expression and autophagy activation in HCC

In the cancer cells of 102 HCC resected tissues, LC3 immunoreactivity was observed in the cytoplasm in 49 of 102 specimens (Fig. 1a). LC3 immunoreactivity was not observed in noncancerous lesions in any specimens. Western blot analysis using a limited set of tissue samples consisting of four matched noncancerous and HCC tissues revealed that expression of LC3-II, a well-known marker of activated autophagy, was detected in the cancerous tissue of case 3 and 4, in which LC3 immunoreactivity was immunohistochemically observed in the cancer cells (Fig. 1b). p62 regulates ubiquitin-positive protein aggregates caused by autophagic deficiency. Considering the results that the expression of p62 were higher in Case 1 and 2 than in Case 3 and 4 both at the cancerous and noncancerous tissues, it also indicated that the autophagic activity were impaired even in the noncancerous tissue and highly impaired in cancerous lesions in the Case 1 and 2.

Relationship between LC3 expression and clinicopathological factors

The positive LC3 expression group had significantly higher serum tumor markers, AFP ($P = 0.0467$) and DCP ($P = 0.0454$), tumor size ($P = 0.0006$) and positive rates of portal vein invasion ($P = 0.0001$) than the negative LC3 expression group (Table 1). Unexpectedly, there were no correlation between the LC3 expression and viral infection. Some patients with HCV or HBV underwent the each pharmacological therapy such as interferon or nucleotide analog, therefore, the activities of hepatitis were difficult to be assessed accurately. That might be the reason why the autophagic activity was necessarily correlated with the presence of the hepatitis clinically.

Association of LC3 with HIF1α expression and HCC recurrence according to HCC tumor size

LC3 (Fig. 1c, $P = 0.0131$) and HIF1α (Fig. 1d, $P = 0.0089$) expression was correlated with tumor size. In the group with a tumor size of ≥3 cm (Fig. 1e), LC3 expression in the high HIF1α expression group was greater than in the low HIF1α expression group ($P = 0.0097$). In any case, LC3 expression in the positive recurrence group was higher than in the negative recurrence group (Fig. 1f, $P = 0.0088$), whereas, in the group with a tumor size of <3 cm, there was no difference in LC3 expression between the high- and low-HIF1α expression groups (Fig. 1g, h). These indicated that only in the case of larger tumors, in which hypoxia and poor nutritional conditions were indicated, the autophagic gene LC3 was highly expressed and that autophagy enhanced tumor growth and promoted HCC malignancy.

Association of high expression of LC3 with tumor size and poor HCC prognosis

For the entire patient group ($n = 131$), the disease-free survival rates of the positive LC3 group (49.0 % at 3 years and 34.7 % at 5 years) was lower than for the negative LC3 group (60.4 % at 3 years and 46.8 % at 5 years) ($P = 0.0056$) (Fig. 2a). In patients with a tumor size of

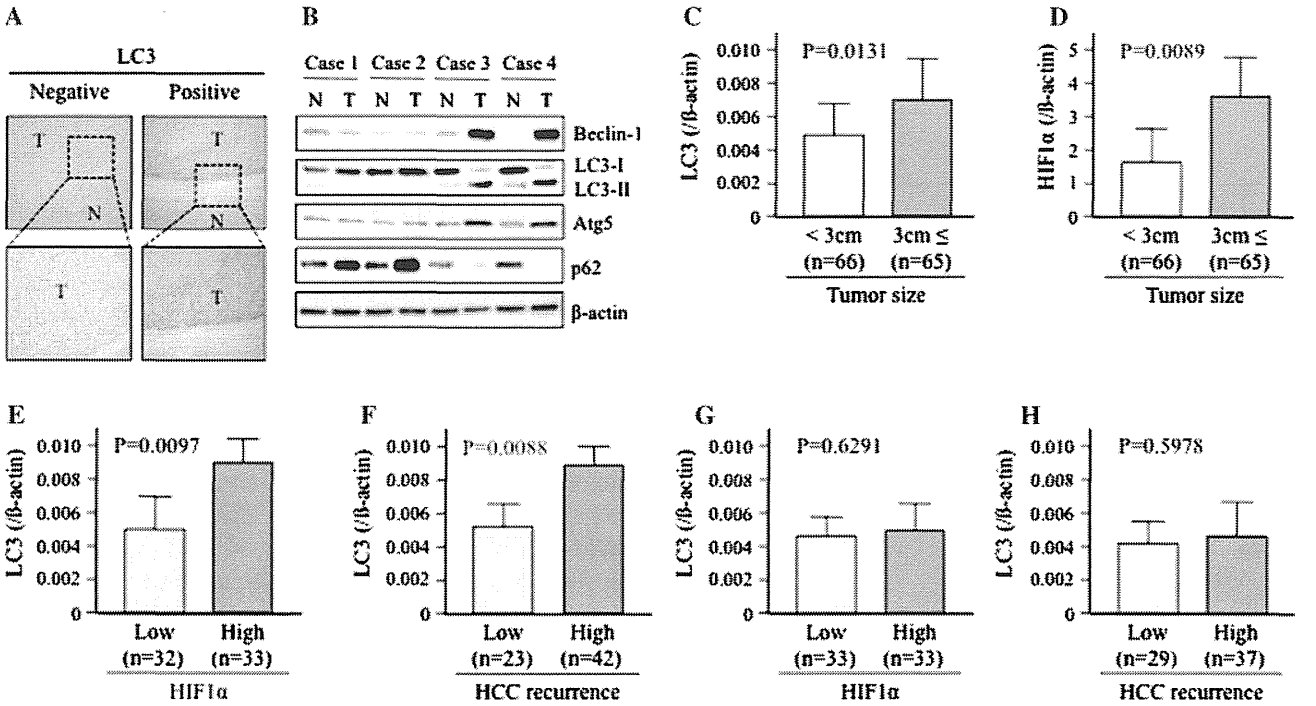

Fig. 1 Upregulation of LC3 protein in HCC human tissue samples (**a**, **b**) and LC3 and HIF1α expression associated with HCC tumor size (**c**–**f**). **a** LC3 immunoreactivity was observed in the cytoplasm of cancer cells, and hepatocytes in non-cancerous tissues were negative for LC3. **b** Western blot analysis of LC3 expression in the four matched HCC tissues and noncancerous tissues. Expression of LC3-II was detected in cancerous tissue in case 3 and 4, but no or only a faint signal was detected in non-cancerous tissue all of the cases. The expression of p62 was higher in case 1 and 2 than in case 3 and 4. **c**–**f** LC3 and HIF1α expression were evaluated by real-time PCR analysis of human HCC samples on the three cohorts: **c**, **d** the total patient population ($n = 131$); **e**, **f** patients with tumor sizes of ≥3 cm ($n = 65$); and **g**, **h** patients with tumor sizes of <3 cm ($n = 66$). They were also divided into two groups consisting of those with high and low expression of HIF1α with a cutoff value with a median of 2.85. LC3 (**c**) and HIF1α (**d**) expression was significantly correlated with tumor size (LC3, $P = 0.0131$; HIF1α, $P = 0.0089$). **e**, **f** In the group with a tumor size of ≥3 cm, LC3 expression in the high HIF1α expression group was significantly greater than that in low HIF1α expression group ($P = 0.0097$) and LC3 expression in the positive recurrence group was significantly higher than in the negative recurrence group ($P = 0.0088$). **g**, **h** In the group with a tumor size of <3 cm, there was no significant difference in LC3 expression between the high and low HIF1α expression groups, and between positive and negative recurrence groups. HCC, hepatocellular carcinoma; HIF1α, hypoxia-induced factor 1α; LC3, microtubule-associated protein 1 light chain 3

≥3 cm ($n = 65$), disease-free survival in the positive LC3 group (48.4 % at 3 years and 32.3 % at 5 years) was lower than in the negative LC3 group (82.6 % at 3 years and 59.8 % at 5 years) ($P = 0.0054$) (Fig. 2b). In contrast, in patients with a tumor size of <3 cm ($n = 66$), there was no difference (Fig. 2c).

Prognostic value of LC3 expression in HCC patients with a tumor size of ≥3 cm

The prognostic factors were evaluated in patients with a tumor size of ≥3 cm using univariate analysis (Table S3), which showed that three parameters namely, ICG R15 ($P = 0.0001$), multiple tumors ($P = 0.0416$) and portal vein invasion ($P = 0.0280$) were predictors of HCC recurrence. Positive LC3 expression was also a predictor of tumor recurrence ($P = 0.0103$). Furthermore, multivariate analysis was conducted with four of the variables (positive LC3 expression, ICG R15 ≥ 14.5 % as median values, multiple tumors and portal vein invasion), and there was no obvious correlation between them (Table 2). Positive LC3 expression was still the independent variable for predicting poor disease free survival ($P = 0.0065$).

Upregulation of LC3 expression in HCC cell lines under hypoxic conditions

Hypoxia markedly increased the number of autophagic vacuoles in Huh7 cells, which appeared as dot-like signals by immunofluorescence analysis (Fig. 3a, b) and electron microscopy (Fig. 3c, d). Expression of LC3-II increased in a time dependent manner (Fig. 3e). These initial observations indicated that HCC cell lines had the potential power to express autophagic activity in response to hypoxic conditions.

Table 1 Immunohistochemical analysis of the correlation between LC3 expression and clinicopathologic characteristics in patients

Variables	LC3 expression (n = 102)		P value
	Negative (n = 53)	Positive (n = 49)	
Age (years)	65 ± 9	62 ± 10	0.1703
Gender (male, %)	77.4	83.7	0.4206
HBs-Ag positive (%)	18.9	22.5	0.6551
HCV-Ab positive (%)	66.0	59.2	0.4744
Serum albumin (g/dL)	4.0 ± 0.4	4.0 ± 0.4	0.3922
Serum T-Bil (mg/dL)	0.9 ± 0.3	0.9 ± 0.3	0.9179
PT (%)	84.1 ± 17.2	87.2 ± 15.5	0.3881
AST (units/L)	49.9 ± 31.0	50.8 ± 24.8	0.8695
ALT (units/L)	51.3 ± 33.7	57.8 ± 51.0	0.4514
ICG R15 (%)	17.0 ± 9.1	15.9 ± 8.7	0.5286
Platelet (10^4/μL)	14.6 ± 7.9	14.9 ± 6.3	0.8053
Child-Pugh A/B, C (%)	86.3/13.7	82.1/17.9	0.5857
Serum AFP (ng/mL)	215 ± 568	14908 ± 63219	0.0468
Serum DCP (mAU/L)	1884 ± 7253	6284 ± 17143	0.0454
Liver cirrhosis (%)	23.5	20.4	0.7062
Tumor size (cm)	3.0 ± 0.4	5.0 ± 0.4	0.0006
Multiple tumors (%)	28.3	38.8	0.2620
Stage I, II/III, IV (%)	66.0/34.0	59.2/40.8	0.4744
Differentiation			
Well, moderate/poor (%)	75.5/24.5	61.2/38.8	0.1207
Portal vein invasion (%)	26.4	69.4	0.0001
Intrahepatic metastasis (%)	13.2	33.3	0.1520

Data are expressed as the mean ± standard deviation

AFP Alpha-fetoprotein, *ALT* alanine aminotransferase, *AST* aspartate aminotransferase, *DCP* des-gamma-carboxyl prothrombin, *HBs-Ag* hepatitis B surface antigen, *HCC* hepatocellular carcinoma, *HCV-Ab* hepatitis C virus antibody, *ICG R15* indocyanine green retention rate at 15 min, *LC3* microtubule-associated protein 1 light chain 3, *PT* prothrombin time, *T-Bil* total bilirubin

Suppression of autophagy and proliferation of HCC cells under hypoxic conditions

LC3 expression was suppressed using two methods namely, pharmacological inhibition by means of 3MA and transfection of $Atg4B^{C74A}$, which involved type III PI3K inhibition and hampering of the conversion of LC3-I to LC3-II, respectively (Fig. S1). Subsequently, the down-regulation of autophagy under hypoxia inhibited the proliferation of HCC cells (Fig. 4a). In addition, the growth of Huh7 cells transfected with GFP-LC3 was higher than the cells receiving no treatment under hypoxic condition (Fig. 4a). These findings indicated that hypoxia-induced autophagy in HCC cells works to promote cell proliferation through preventing accumulation of damaged protein and organelles.

Suppression of autophagy activity and mitochondrial β-oxidation

The levels of intracellular ATP in autophagy-inhibited HCC cells were lower than in non-treated cells (Fig. 4b). The proportion of HCC cells with low mitochondria membrane permeability treated with autophagy-inhibitor was higher (Fig. 4c). Gene expression levels of MCAD and CPT, L-FABP, and FATP enzymes in autophagy-inhibited cells, which were indicated to have a rate-controlling effect on β-oxidation, the transportation of free fatty acids to mitochondria, and the transport of free fatty acids into hepatocytes, respectively, were significantly lower than those in non-treated cells (Fig. 4d). Consequently, β-hydroxybutyrate levels, final ketone body product, in autophagy-inhibited cells were decreased more than in non-treated cells (Fig. 4e). These findings indicated that HCC cells exposed to hypoxia had the potential power to maintain intracellular ATP through the activation of mitochondrial β-oxidation, which may have been due to the prompt removal of the damaged mitochondria by activated autophagy as a selective degradation system.

Discussion

In the present study, the inalterable role of autophagy in human HCC exposed to hypoxic conditions as tumors grew in size was demonstrated. The LC3 expression was correlated with tumor size, and only in large tumors, was correlated with the expression of HIF1α, hypoxia and the under nutrition marker. Additionally, high expression of LC3 was shown to be an independent predictor of HCC recurrence. Further, analysis of HCC cell lines using autophagy-inhibitor revealed that the hypoxia-induced autophagy in HCC cells worked to promote cell proliferation through maintenance of intracellular ATP. This depended on the activation of mitochondrial β-oxidation with the prompt removal of damaged mitochondria due to activated autophagy. This is the first report demonstrating the mechanism involved in maintaining the intracellular energy sources by means of activated autophagy, as HCC tumors developed in large size under hypoxic stress. Recently some reports demonstrated that the emerging role of autophagy for promoting cell viability in HCC progressions during ischemia-hypoxia condition only in the rodent models [29, 30]. We also demonstrated these results even in human samples clinically and emphasized that 'only in the large tumors' in which the impact of hypoxia and poor conditions were involved, the autophagic activity

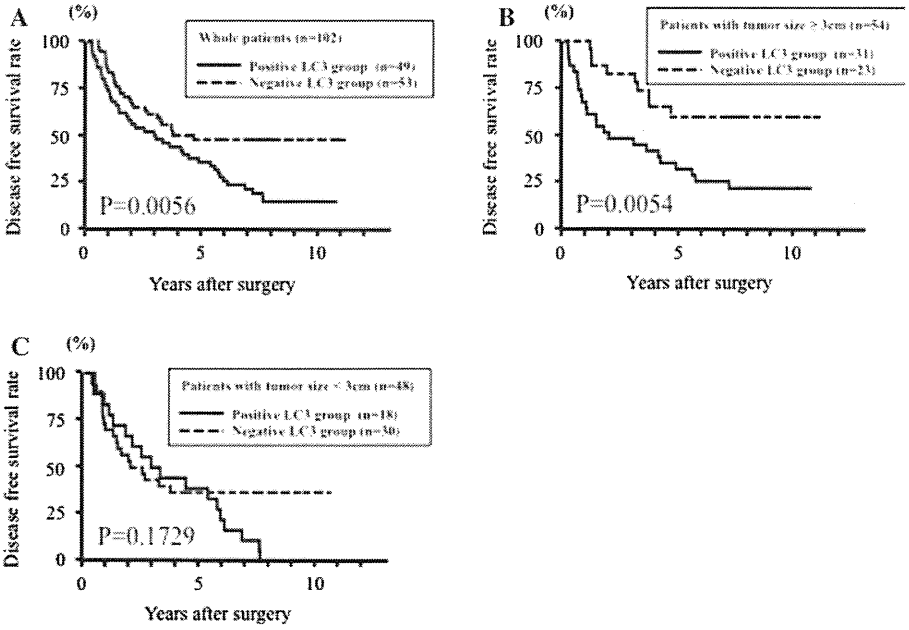

Fig. 2 Association between LC3 expression and patients' prognosis depending on tumor size of HCC. The disease-free survival after surgery were compared between the positive and negative LC3 expression groups by immunohistochemical analysis. The analysis was performed on three cohorts: **a** the total patient group ($n = 102$); **b** patients with tumor sizes of ≥3 cm ($n = 54$); and **c** patients with tumor sizes of <3 cm ($n = 48$). **a** For the entire patient group, the disease-free survival rates of the positive LC3 group (49.0 % at 3 years and 34.7 % at 5 years) was significantly lower than that of the negative LC3 group (60.4 % at 3 years and 46.8 % at 5 years) ($P = 0.0056$). **b** In the patients with a tumor size of ≥3 cm, disease-free survival in the positive LC3 group (48.4 % at 3 years and 32.3 % at 5 years) was significantly lower than in the negative LC3 group (82.6 % at 3 years and 59.8 % at 5 years) ($P = 0.0054$). **c** In patients with a tumor size of <3 cm there was no significant difference between the two groups. *HCC* hepatocellular carcinoma, *LC3* microtubule-associated protein 1 light chain 3

Table 2 Multivariate analysis of risk factors related to postoperative recurrence in patients with HCC tumors of ≥3 cm

Variables ($n = 75$)	Odds ratio	95 % CI	P value
ICG R15 ≥ 14.5 (%)	6.306	2.471–22.704	0.0001
LC3 Positive vs. negative	2.962	1.333–7.841	0.0065
Multiple tumors Positive vs. negative	2.626	1.152–7.210	0.0202
Portal vein invasion Positive vs. negative	2.200	1.012–5.439	0.0465

CI Confidence interval, *HCC* hepatocellular carcinoma, *ICG R15* indocyanine green retention rate at 15 min, *LC3* microtubule-associated protein 1 light chain 3

was highly expressed and its enhancement for the tumor growth and promotion of HCC malignancy, therefore, the newly targeted therapy for autophagy pathway of these adaptive metabolic responses is desired to becomes major challenges to overcome the large sized HCC tumors.

The role of autophagy in cell fate decision remains controversial. Autophagy is claimed to be an indispensable physiological reaction that sustains cell viability under nutrient-starved conditions [31]. Regarding cancer cells, it has been reported that autophagy was highly expressed in many of these cells and that this high expression was a strong factor related to tumor progression [32]. However, autophagy has recently attracted attention in connection with programmed or autophagic cell death. Colell et al. [33] demonstrated that cell death resulting from progressive cellular consumption can be attributed to unrestrained autophagy, which has led to the belief that autophagy is a nonapoptotic form of programmed cell death [34, 35]. However, the role of autophagy, an alternative caspase-independent cell death program, and its underlying molecular mechanism, is still controversial in cancer, especially in tumor progression. About the mTOR pathway, mTOR inhibitors such as RAD001, also an autophagy inducer, does not promote the proliferation of HCC cells and results in cell death [36, 37]. Weiner et al. [38], demonstrated that autophagy is observed in established cancers, but its inhibition during early carcinogenesis actually promotes tumor progression, suggesting that an autophagic switch promotes the transition of a tumor into a state of so-called autophagy addiction in order to maintain viability in hypoxic, nutrient-limited microenvironments. They also discussed that the autophagic function depends on the extent to which cells are capable of enhancing basal levels of autophagy. In fact, the hyperdynamic state of autophagy might be the crisis of cellular life because of its

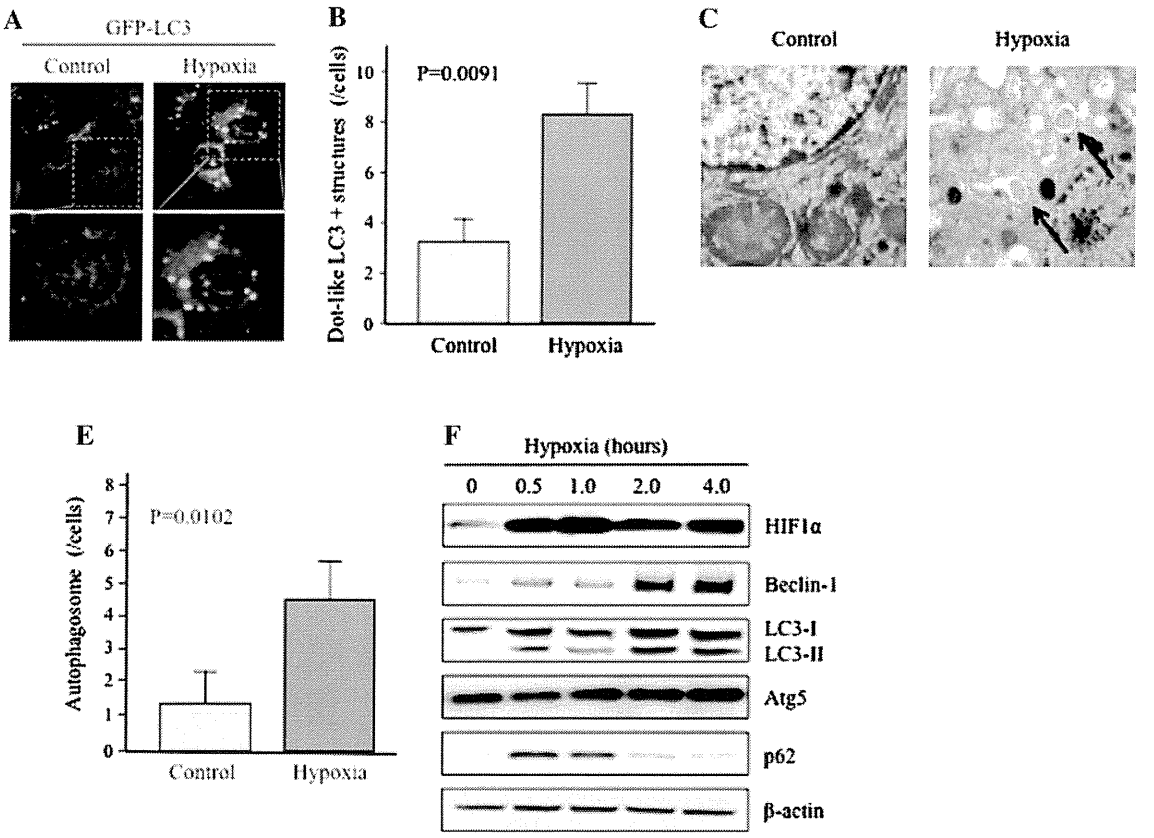

Fig. 3 Upregulation of LC3 protein in HCC cell lines under hypoxic conditions. **a**, **b** Huh7 cells exposed to 2 h hypoxic conditions had markedly increased numbers of autophagic vacuoles, which appeared as dot-like signals by immunofluorescence analysis using antibody against LC3. **c**, **d** Extensive autophagosome formation (*arrowed*) in Huh7 cells exposed to 2 h hypoxic conditions was monitored using electron microscopy. **e** The expression of LC3-II increased in a time-dependent manner when evaluated by western blot analysis using the proteins extracted from Huh7 cells under hypoxic conditions for the indicated times. The expression of the other autophagic genes, Beclin-1 and Atg5, also increased in a time-dependent manner. *Atg* Autophagy-related genes, *HCC* hepatocellular carcinoma, *LC3* microtubule-associated protein 1 light chain 3

consumption of the intracellular even healthy organelle and proteins. Considering the reports of mTOR inhibitors resulted in HCC cell death, the basal levels of autophagy in these setting of HCC cells and whether its inhibitor might excessively induce the autophagic activity or not should be carefully assessed because mTOR is a strong key component in a series of pathways involved in tumor growth and development. We revealed the protective role played by autophagy that involves proliferation of HCC cells due to activation of mitochondrial β-oxidation. Furthermore, we investigated the clinical significance of this finding regarding the link between autophagy and tumor progression. Three HIF1α-dependent molecular mechanisms have been reported by which cells adapt their energy metabolism under hypoxic conditions: inhibition of mitochondrial biogenesis by repression of c-Myc activity [39]; inhibition of acetyl-CoA synthesis by activation of PDK1 [40], and COX4 subunit switching [41]. We demonstrated that protection of mitochondria by autophagy is a fourth component of the HIF1α-mediated metabolic adaptation required to prevent cell death and damaged mitochondria, due to increased ROS levels in HCC cells under low nutrient conditions.

Ding et al. [42] demonstrated that only in an apoptosis compromised background, the expression of the autophagic gene, Beclin 1, and their corresponding autophagic activities were suppressed in HCC. They indicated that the loss of a survival pathway, autophagy, enhanced tumor growth by promoting genome damage and instability in an apoptosis-deficient background, a Bcl-xL positive background. However, their data depended on the assessment of the expression of Beclin-1 and there were multiple molecular machineries involved in the formation of the autophagosome downstream of Beclin-1. Therefore, it was not established whether autophagy was truly activated [39]. Recently, some reports demonstrated Beclin-1 independent autophagy, which acted as a caspase-independent cell death mechanism [43–45]. Additionally, Beclin-1 is the multifunctional gene involved in apoptosis [46, 47]. Thus, Beclin-1 plays a key role in autophagy,

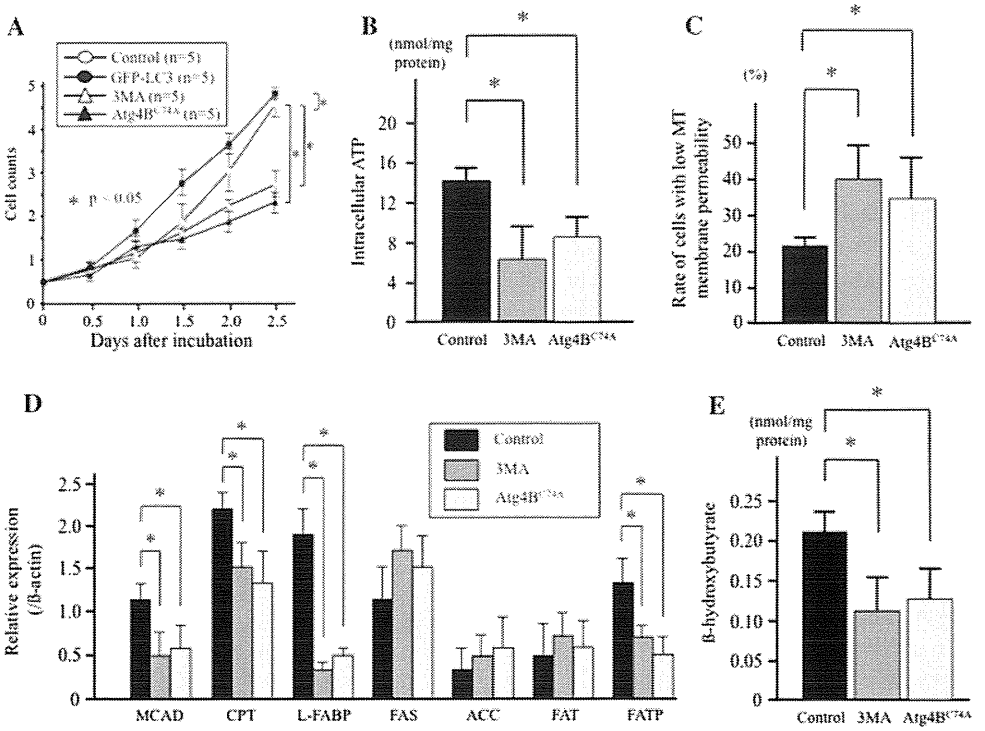

Fig. 4 Impaired proliferation of HCC cell lines treated with autophagy-inhibitor and deterioration of intracellular ATP maintenance through impairment of mitochondrial β-oxidation due to suppressed autophagy activity. Huh7 cells receiving no treatment or treated with autophagy-inhibitor using two methods, pharmacological inhibitor as 3MA and transfection of Atg4B^{C74A}, were incubated under hypoxic conditions of 0.1 % O_2 final concentration for 2 h. **a** Growth of both Huh7 cells treated using the two methods of autophagy-inhibition were significantly lower than that of the cells receiving no treatment under hypoxic conditions. In addition, the growth of Huh7 cells transfected with GFP-LC3 was higher than the cells receiving no treatment under hypoxic condition. **b** The intracellular ATP in the Huh7 cells treated with autophagy-inhibitor under hypoxic conditions was present at significantly lower levels than in cells receiving no treatment. **c** The proportion of Huh7 cells with low levels of mitochondrial membrane permeability treated with autophagy-inhibitor was higher than that of non-treated cells by by FACScan analysis using JC-1 antibody. **d** The gene expression related to mitochondrial β-oxidation in Huh7 cells were examined by real-time PCR. The levels of the enzymes MCAD and CPT, L-FABP, and FATP in Huh7 cells treated with autophagy-inhibitor were significantly lower than that in non-treated cells. **e** The intracellular β-hydroxybutyrate levels in Huh7 cells treated with autophagy-inhibitor under hypoxic conditions were significantly lower than in cells receiving no treatment. *ACC* Acetyl-CoA carboxylase, *ATP* adenosine 5′-triphosphate, *CPT* carnitine palmitoyltransferase, *FAS* fatty acid synthase, *FAT* fatty acid translocase, *FATP* fatty acid transport protein, *L-FABP* fatty acid binding protein, *LC3* microtubule-associated protein 1 light chain 3, *MCAD* medium-chain acyl-CoA dehydrogenase, *PCR* polymerase chain reaction, *3MA* 3-methyladenine

however, Beclin-1 should be carefully analyzed for the assessment of activated autophagy. The standard method for assessing autophagic activity is the demonstration of autophagic vesicles using electron microscopy, [48] and another method is the LC3-based assay. When autophagy occurs, conversion of a fraction of the cytosolic form of LC3-I to the autophagic membrane form of LC3-II can be detected using western blots of LC3 proteins. This change in intracellular localization of LC3 protein is considered to correlate with autophagic activity [49], and LC3 expression detected using immunohistochemistry represents the steady-state LC3 level including both LC3-I and LC3-II. We examined activated autophagy promptly with LC3-II using western blotting and confirmed the high expression of autophagosomes using an electron microscope.

Regarding the energy supply system in surviving cancer cells, several cancer cell lines including pancreatic cancer-derived and colorectal cancer-derived cell lines, are resistant to nutrient-deprived culture conditions [50]. These cells might use some alternative metabolic process to obtain energy for survival. However, untransformed human fibroblasts were completely abolished under the same conditions [51]. These indicated that this phenomenon of starvation-resistance may contribute to survival of cancer cells in nutrient-deficient microenvironments. As an alternative energy source, mammalian cells can use amino acids [52]. If the starvation-resistant cancer cells can raise amino acids from the inside of cells, these amino acids become potential energy sources. Autophagy is an evolutionarily conserved process involving lysosomal degradation of cytoplasmic and cellular organelles

[11, 26]. Autophagy constitutes a stress adaptation that avoids tumor death and has roles in protecting cells against the shortage of nutrients [26, 53]. Furthermore, autophagy is a catabolic process by which cells supply amino acids from self-digested organelles, as an alternative energy source for survival [11, 13, 31]. This function of autophagy seems ideal in fostering the survival of cancer cells in an unfavorable starved microenvironment. We demonstrated that autophagy plays an essential role by maintaining an optimal balance between the competing demands of energy and proliferation under hypoxic conditions. Whereas consideration of cellular energetics favors oxidative metabolism as the most efficient means of producing adequate levels of ATP to maintain cell survival, mitochondrial respiration is also associated with increased amino acid consumption due to autophagy. It was reasonable that the two aspects of HIF1α mediated-autophagic function, namely the protection of mitochondria and the supply amino acids from inside the cell contributed to cell survival in response to hypoxia.

For the recurrence of HCC after surgery, high expression of LC3 is the independent predictive factor in the context of larger sized tumors. Other predictive factors were liver dysfunction defined as ICG R15 < 14.5 %, multiple tumors and portal vein invasion. As HCC tumors grow, it becomes difficult to secure an exogenous energy supply, in particular for the central nest of tumors. However, in small HCC tumors with adequate oxygen supply and enriched nutrient conditions, cells did not struggle to obtain energy from an exogenous nutrient supply. For this reason, in patients with tumors of <3 cm, there was no correlation between LC3 expression, and HIF1α expression and tumor size. However, in patients with tumors of ≥3 cm, LC3 expression was significantly associated with HIF1α expression. To curatively treat HCC, an effective approach may be not only to inhibit the autophagy machinery, but also the HIF1α machinery molecule to prevent energy supply in conditions in which exogenous nutrient supply is extremely limited.

We have provided experimental evidence supporting the conclusion that HIF1α-mediated autophagy is involved in mitochondrial metabolism and is essential to understanding the mechanisms and consequences of the maintenance of intracellular energy in cancer cells under hypoxic conditions. This process requires the HIF1α-dependent induction of autophagy machinery as demonstrated by means of LC3-deficient HCC cell analysis. Understanding the factors determining which of these adaptive metabolic responses to conditions of hypoxia and under nutrition in HCC cells are utilized in vitro and in vivo, and whether these adaptations are successful in preventing cell death, remains a challenge.

Acknowledgments We are grateful to T. Yoshimori (Osaka University) for kindly providing the inactive mutant of Atg4B ($Atg4B^{C74A}$). We also thank N. Yamashita (Kyushu University) for her expert advice related to statistical analysis.

Conflict of interest The authors have no conflicts of interest to declare and have no financial interests linked to this work.

References

1. Shirabe K, Toshima T, Taketomi A, et al. Hepatic aflatoxin B1-DNA adducts and TP53 mutations in patients with hepatocellular carcinoma despite low exposure to aflatoxin B1 in southern Japan. Liver Int. 2011;31:1366–72.
2. Shirabe K, Itoh S, Yoshizumi T, et al. The predictors of microvascular invasion in candidates for liver transplantation with hepatocellular carcinoma-with special reference to the serum levels of des-gamma-carboxy prothrombin. J Surg Oncol. 2007;95:235–40.
3. Shirabe K, Kajiyama K, Harimoto N, Tsujita E, Wakiyama S, Maehara Y. Risk factors for massive bleeding during major hepatectomy. World J Surg. 2010;34:1555–62.
4. Bruix J, Llovet JM. Prognostic prediction and treatment strategy in hepatocellular carcinoma. Hepatology. 2002;35:519–24.
5. Yamashita Y, Taketomi A, Shirabe K, et al. Outcomes of hepatic resection for huge hepatocellular carcinoma (≥10 cm in diameter). J Surg Oncol. 2011;104:292–8.
6. Taketomi A, Sanefuji K, Soejima Y, et al. Impact of des-gamma-carboxy prothrombin and tumor size on the recurrence of hepatocellular carcinoma after living donor liver transplantation. Transplantation. 2009;87:531–7.
7. Vaupel P, Thews O, Hoechkel M. Treatment resistance of solid tumors: role of hypoxia and anemia. Med Oncol. 2001;18:243–59.
8. Jain RK. Molecular regulation of vessel maturation. Nat Med. 2003;9:685–93.
9. Harris AL. Hypoxia—a key regulatory factor in tumour growth. Nat Rev Cancer. 2002;2:38–47.
10. Kitano M, Kudo M, Maekawa K, et al. Dynamic imaging of pancreatic diseases by contrast enhanced coded phase inversion harmonic ultrasonography. Gut. 2004;53:854–9.
11. Klionsky DJ, Emr SD. Autophagy as a regulated pathway of cellular degradation. Science. 2000;290:1717–21.
12. Tanida I, Tanida-Miyake E, Ueno T, Kominami E. The human homolog of *Saccharomyces cerevisiae* Apg7p is protein-activating enzyme for multiple substrates including human Apg12p, GATE-16, GABARAP, and MAP-LC3. J Biol Chem. 2001;276:1701–6.
13. Mizushima N, Yoshimori T, Levine B. Methods in mammalian autophagy research. Cell. 2010;140:313–26.
14. Fleming A, Noda T, Yoshimori T, Rubinsztein DC. Chemical modulators of autophagy as biological probes and potential therapeutics. Nat Chem Biol. 2011;7:9–17.
15. Liver Cancer Study Group. The general rules for the clinical and pathological study of primary liver cancer. 7th ed. Tokyo: Kanehara Publications; 2006.
16. Fujita N, Hayashi-Nishino M, Fukumoto H, et al. An Atg4B mutant hampers the lipidation of LC3 paralogues and causes defects in autophagosome closure. Mol Biol Cell. 2008;19:4651–9.
17. Aishima S, Fujita N, Mano Y, et al. Different roles of S100P overexpression in intrahepatic cholangiocarcinoma: carcinogenesis

of perihilar type and aggressive behavior of peripheral type. Am J Surg Pathol. 2011;35:590–8.
18. Kabeya Y, Mizushima N, Yamamoto A, Oshitani-Okamoto S, Ohsumi Y, Yoshimori T. LC3, GABARAP and GATE16 localize to autophagosomal membrane depending on form-II formation. J Cell Sci. 2004;117:2805–12.
19. Mizushima N, Yoshimori T, Levine B. Methods in mammalian autophagy research. Cell. 2010;140:313–26.
20. Klionsky DJ, Abdalla FC, Abeliovich H, Abraham RT, Acevedo-Arozena A, Adeli K, et al. Guidelines for the use and interpretation of assays for monitoring autophagy. Autophagy. 2012;8: 445–544.
21. Anegawa G, Kawanaka H, Yoshida D, et al. Defective endothelial nitric oxide synthase signaling is mediated by rho-kinase activation in rats with secondary biliary cirrhosis. Hepatology. 2008;47:966–77.
22. Sadagurski M, Cheng Z, Rozzo A, et al. IRS2 increases mitochondrial dysfunction and oxidative stress in a mouse model of Huntington disease. J Clin Invest. 2011;121:4070–81.
23. Nanjundan M, Nakayama Y, Cheng KW, et al. Amplification of MDS1/EVI1 and EVI1, located in the 3q26.2 amplicon, is associated with favorable patient prognosis in ovarian cancer. Cancer Res. 2007;67:3074–84.
24. Klionsky DJ, Abeliovich H, Agostinis P, Agrawal DK, Aliev G, Askew DS, et al. Guidelines for the use and interpretation of assays for monitoring autophagy in higher eukaryotes. Autophagy. 2008;4:151–75.
25. Kasahara A, Ishikawa K, Yamaoka M, et al. Generation of trans-mitochondrial mice carrying homoplasmic mtDNAs with a missense mutation in a structural gene using ES cells. Hum Mol Genet. 2006;15:871–81.
26. Du H, Yang W, Chen L, Shen B, Peng C, Li H, et al. Emerging role of autophagy during ischemia-hypoxia and reperfusion in hepatocellular carcinoma. Int J Oncol. 2012;40:2049–57.
27. Chang Y, Yan W, He X, Zhang L, Li C, Huang H, et al. miR-375 inhibits autophagy and reduces viability of hepatocellular carcinoma cells under hypoxic conditions. Gastroenterology. 2012; 143:177–87.
28. Petit PX, et al. Alterations in mitochondrial structure and function are early events of dexamethasone-induced thymocyte apoptosis. J Cell Biol. 1995;130:157–67.
29. Hanson GT, Aggeler R, Oglesbee D, et al. Investigating mitochondrial redox potential with redox-sensitive green fluorescent protein indicators. J Biol Chem. 2004;279:13044–53.
30. Aleksunes LM, Reisman SA, Yeager RL, Goedken MJ, Klaassen CD. Nuclear factor erythroid 2-related factor 2 deletion impairs glucose tolerance and exacerbates hyperglycemia in type 1 diabetic mice. J Pharmacol Exp Ther. 2010;333:140–51.
31. Levine B, Klionsky DJ. Development by self-digestion: molecular mechanisms and biological functions of autophagy. Dev Cell. 2004;6:463–77.
32. Kuwahara Y, Oikawa T, Ochiai Y, et al. Enhancement of autophagy is a potential modality for tumors refractory to radiotherapy. Cell Death Dis. 2011;2:e177.
33. Colell A, Ricci JE, Tait S, et al. GAPDH and autophagy preserve survival after apoptotic cytochrome c release in the absence of caspase activation. Cell. 2007;129:983–7.
34. Kirkegaard K, Taylor MP, Jackson WT. Cellular autophagy: surrender, avoidance and subversion by microorganisms. Nat Rev Microbiol. 2004;2:301–14.
35. Kondo Y, Kanzawa T, Sawaya R, Kondo S. The role of autophagy in cancer development and response to therapy. Nat Rev Cancer. 2005;5:726–34.
36. Thomas HE, Mercer CA, Carnevalli LS, Park J, Andersen JB, Conner EA, et al. mTOR inhibitors synergize on regression, reversal of gene expression, and autophagy in hepatocellular carcinoma. Sci Transl Med. 2012;4:139ra84.
37. Altmeyer A, Josset E, Denis JM, Gueulette J, Slabbert J, Mutter D, Noël G, Bischoff P. The mTOR inhibitor RAD001 augments radiation-induced growth inhibition in a hepatocellular carcinoma cell line by increasing autophagy. Int J Oncol. 2012. doi: 10.3892/ijo.2012.1583.
38. Weiner LM, Lotze MT. Tumor-cell death, autophagy, and immunity. N Engl J Med. 2012;366:1156–8.
39. Lu Z, Dono K, Gotoh K, et al. Participation of autophagy in the degeneration process of rat hepatocytes after transplantation following prolonged cold preservation. Arch Histol Cytol. 2005;68:71–80.
40. Degenhardt K, Mathew R, Beaudoin B, et al. Autophagy promotes tumor cell survival and restricts necrosis, inflammation, and tumorigenesis. Cancer Cell. 2006;10:51–64.
41. Pouyssegur J, Dayan F, Mazure NM. Hypoxia signalling in cancer and approaches to enforce tumour regression. Nature. 2006;441:437–43.
42. Ding ZB, Shi YH, Zhou J, et al. Association of autophagy defect with a malignant phenotype and poor prognosis of hepatocellular carcinoma. Cancer Res. 2008;68:9167–75.
43. Scarlatti F, Maffei R, Beau I, Codogno P, Ghidoni R. Role of non-canonical Beclin 1-independent autophagy in cell death induced by resveratrol in human breast cancer cells. Cell Death Differ. 2008;15:1318–29.
44. Chu CT, Zhu J, Dagda R. Beclin 1-independent pathway of damage-induced mitophagy and autophagic stress: implications for neurodegeneration and cell death. Autophagy. 2007;3:663–6.
45. Pickford F, Masliah E, Britschgi M, et al. The autophagy-related protein beclin 1 shows reduced expression in early Alzheimer disease and regulates amyloid beta accumulation in mice. J Clin Invest. 2008;118:2190–9.
46. Boya P, González-Polo RA, Casares N, et al. Inhibition of macroautophagy triggers apoptosis. Mol Cell Biol. 2005;25: 1025–40.
47. Ait-Mohamed O, Battisti V, Joliot V, et al. Acetonic extract of *Buxus sempervirens* induces cell cycle arrest, apoptosis and autophagy in breast cancer cells. PLoS One. 2011;6:e24537.
48. Mizushima N, et al. Methods for monitoring autophagy. Int J Biochem Cell Biol. 2004;36:2491–502.
49. Kabeya Y, Mizushima N, Ueno T, et al. LC3, a mammalian homologue of yeast Apg8p, is localized in autophagosome membranes after processing. EMBO J. 2000;19:5720–8.
50. Sato K, Tsuchihara K, Fujii S, et al. Autophagy is activated in colorectal cancer cells and contributes to the tolerance to nutrient deprivation. Cancer Res. 2007;67:9677–84.
51. Esumi H, Izuishi K, Kato K, et al. Hypoxia and nitric oxide treatment confer tolerance to glucose starvation in a 5′-AMP-activated protein kinase-dependent manner. J Biol Chem. 2002;277:32791–8.
52. Kuma A, Hatano M, Matsui M, et al. The role of autophagy during the early neonatal starvation period. Nature. 2004;432: 1032–6.
53. Rouschop KM, van den Beucken T, Dubois L, et al. The unfolded protein response protects human tumor cells during hypoxia through regulation of the autophagy genes MAP1LC3B and ATG5. J Clin Invest. 2010;120:127–41.

Stem Cell Reports
Resource
ISSCR
OPEN ACCESS

Long-Term Self-Renewal of Human ES/iPS-Derived Hepatoblast-like Cells on Human Laminin 111-Coated Dishes

Kazuo Takayama,[1,2,3] Yasuhito Nagamoto,[1,2] Natsumi Mimura,[2] Katsuhisa Tashiro,[4] Fuminori Sakurai,[1] Masashi Tachibana,[1] Takao Hayakawa,[5] Kenji Kawabata,[4] and Hiroyuki Mizuguchi[1,2,3,6,*]
[1]Laboratory of Biochemistry and Molecular Biology, Graduate School of Pharmaceutical Sciences, Osaka University, Osaka 565-0871, Japan
[2]Laboratory of Hepatocyte Differentiation, National Institute of Biomedical Innovation, Osaka 567-0085, Japan
[3]iPS Cell-Based Research Project on Hepatic Toxicity and Metabolism, Graduate School of Pharmaceutical Sciences, Osaka University, Osaka 565-0871, Japan
[4]Laboratory of Stem Cell Regulation, National Institute of Biomedical Innovation, Osaka 567-0085, Japan
[5]Pharmaceutical Research and Technology Institute, Kinki University, Osaka 577-8502, Japan
[6]The Center for Advanced Medical Engineering and Informatics, Osaka University, Osaka 565-0871, Japan
*Correspondence: mizuguch@phs.osaka-u.ac.jp
http://dx.doi.org/10.1016/j.stemcr.2013.08.006

SUMMARY

The establishment of self-renewing hepatoblast-like cells (HBCs) from human pluripotent stem cells (PSCs) would realize a stable supply of hepatocyte-like cells for medical applications. However, the functional characterization of human PSC-derived HBCs was not enough. To purify and expand human PSC-derived HBCs, human PSC-derived HBCs were cultured on dishes coated with various types of human recombinant laminins (LN). Human PSC-derived HBCs attached to human laminin-111 (LN111)-coated dish via integrin alpha 6 and beta 1 and were purified and expanded by culturing on the LN111-coated dish, but not by culturing on dishes coated with other laminin isoforms. By culturing on the LN111-coated dish, human PSC-derived HBCs were maintained for more than 3 months and had the ability to differentiate into both hepatocyte-like cells and cholangiocyte-like cells. These expandable human PSC-derived HBCs would be manageable tools for drug screening, experimental platforms to elucidate mechanisms of hepatoblasts, and cell sources for hepatic regenerative therapy.

INTRODUCTION

Human embryonic stem cells (hESCs) and human induced pluripotent stem cells (hiPSCs) have the ability to self-replicate and to differentiate into all types of body cells including hepatoblasts and hepatocytes. Although cryopreserved primary human hepatocytes are useful in drug screening and liver cell transplantation, they rapidly lose their functions (such as drug metabolism capacity) and hardly proliferate in in vitro culture systems. On the other hand, human hepatic stem cells from fetal and postnatal human liver are able to self-replicate and able to differentiate into hepatocytes (Schmelzer et al., 2007; Zhang et al., 2008). However, the source of human hepatic stem cells is limited, and these cells are not available commercially. Therefore, the human pluripotent stem cell (hPSC)-derived hepatoblast-like cells (HBCs), which have potential to differentiate into the hepatocyte-like cells, would be an attractive cell source to provide abundant hepatocyte-like cells for drug screening and liver cell transplantation.

Because expandable and multipotent hepatoblasts or hepatic stem cells are of value, suitable culture conditions for the maintenance of hepatoblasts or hepatic stem cells obtained from fetal or adult mouse liver were developed (Kamiya et al., 2009; Tanimizu et al., 2004). Soluble factors, such as hepatocyte growth factor (HGF) and epidermal growth factor (EGF), are known to support the proliferation of mouse hepatic stem cells and hepatoblast (Kamiya et al., 2009; Tanimizu et al., 2004). Extracellular matrix (ECM) also affects the maintenance of hepatoblasts or hepatic stem cells. Laminin can maintain the character of mouse hepatoblasts (Dlk1-positive cells) (Tanimizu et al., 2004). However, the methodology for maintaining HBCs differentiated from hPSCs has not been well investigated. Zhao et al. (2009) have reported that hESC-derived hepatoblast-like cells (sorted N-cadherin-positive cells were used) could be maintained on STO feeder cells. Although a culture system using STO feeder cells for the maintenance of hepatoblast-like cells might be useful, there are two problems. The first problem is that N-cadherin is not a specific marker for human hepatoblasts. N-cadherin is also expressed in hESC-derived mesendoderm cells and definitive endoderm (DE) cells (Sumi et al., 2008). The second problem is that residual undifferentiated cells could be maintained on STO feeder cells. Therefore, their culture condition cannot rule out the possibility of the proliferation of residual undifferentiated cells. Because it is known that hPSC-derived cells have the potential to form teratomas in the host, the production of safer hepatocyte-like cells or hepatoblast-like cells has been required. Therefore, we decided to purify hPSC-derived HBCs, which can differentiate into mature hepatocyte-like cells, and then expand these cells.

In this study, we attempt to determine a suitable culture condition for the extensive expansion of HBCs derived

from hPSCs. We found that the HBCs derived from hPSCs can be maintained and proliferated on human laminin-111 (LN111)-coated dishes. To demonstrate that expandable, multipotent, and safe (i.e., devoid of residual undifferentiated cells) hPSC-derived HBCs could be maintained under our culture condition, the hPSC-derived HBCs were used for hepatic and biliary differentiation, colony assay, and transplantation into immunodeficient mice.

RESULTS

Human PSC-Derived Hepatoblast-like Cells Could Adhere onto Human LN111 via Integrin α6 and β1

The HBCs were generated from hPSCs (hESCs and hiPSCs) as described in Figure 1A (details of the characterization of hPSC-derived HBCs are described in Figure 3). Definitive endoderm differentiation of hPSCs was promoted by stage-specific transient transduction of FOXA2 in addition to the treatment with appropriate soluble factors (such as Activin A). Overexpression of FOXA2 is not necessary for establishing the hPSC-derived HBCs, but it is helpful for efficient generation of the hPSC-derived HBCs. On day 9, these hESC-derived populations contained two cell populations with distinct morphology (Figure 1B). One population resembled human hepatic stem cells that were isolated from human fetal liver (shown in red) (Schmelzer et al., 2007), whereas the other population resembled definitive endoderm cells (shown in green) (Hay et al., 2008). The population that resembled human hepatic stem cells was alpha-1-fetoprotein (AFP) positive, whereas the other population was AFP negative (Figure 1C, left). On day 9, the percentage of AFP-positive cells was approximately 80% (Figure 1C, right). To characterize these two cell populations (hESC-derived HBC and non-HBC [NHBC] populations), the colonies were manually isolated by using a pipette, and then the gene expression analysis was performed. The gene expression levels of *AFP*, *CD133*, *EpCAM*, *CK8*, and *CK18* in the hESC-derived HBCs were higher than those in the bulk population containing both hESC-derived HBCs and NHBCs (*CD133*, *EpCAM*, *CK8*, and *CK18* were named as pan-hepatoblast markers and are known to be strongly expressed in both human hepatic stem cells and hepatoblasts [Schmelzer et al., 2007; Zhang et al., 2008]) (Figure 1D). On the other hand, the gene expressions of *AFP*, *CD133*, *EpCAM*, *CK8*, and *CK18* in the hESC-derived NHBCs were hardly detected. The gene expression levels of DE, mesendoderm, and pluripotent markers in the hESC-derived NHBCs were higher than those in the hESC-derived HBCs, indicating that the hESC-derived NHBCs could remain in a more undifferentiated state than the hESC-derived HBCs (Figures S1A–S1C available online). These results suggest that hepatoblast-like cells could be differentiated from hPSCs.

To purify the hESC-derived HBCs, these cells were plated onto dishes coated with various laminins. There are 15 different laminin isoforms in human tissues. Although laminin is known to be useful to sustain mouse hepatoblasts (Tanimizu et al., 2004), it remains unknown which human laminin isoform has the potential to purify and expand the HBCs. To identify a human laminin isoform that would be useful for purifying hESC-HBCs, the hESC-HBCs and -NHBCs were plated onto dishes coated with various types of commercially available human laminins (Figure 1E). The hESC-derived HBCs could more efficiently adhere onto the human LN111-coated dish compared with hESC-derived NHBCs or unseparated populations (containing both HBCs and NBCs). These data suggest that a hESC-derived HBC population can be purified from the unseparated populations by culturing on human LN111-coated dishes. Because integrins are known to be important molecules for cell adhesion to the ECM including laminins, we expected that certain types of integrins would allow selective adhesion of the hESC-derived HBCs to human LN111-coated dish. The gene expression levels of various integrins were examined (Figure 1F). Among the integrin α subunits, the gene expression level of *integrin α6* in the hESC-derived HBCs was significantly higher than that in the hESC-derived NHBCs. In contrast, among the integrin β subunits, the gene expression level of *integrin β1* was higher than those of *integrin β2* and *β3* in all cell populations. The hESC-derived HBCs, but not NHBCs, expressed both integrin α6 and β1 (Figure S1D). Almost all adhesion of the hESC-derived HBCs to a human LN111-coated dish was inhibited by both function-blocking antibodies to integrin α6 and β1 (Figure 1G). These results indicated that the hESC-derived HBCs could attach to a human LN111-coated dish via integrin α6 and β1.

The hPSC-Derived HBCs Could Be Proliferated and Maintained on a Human LN111-Coated Dish

To obtain the purified hESC-derived HBC population, the hESC-derived cells (day 9) were plated onto a human LN111-coated dish, and then unattached cells were removed at 15 min after plating (Figure 2A). Among various laminins, only human LN111 could proliferate (Figure 2B) and purify (Figure 2C) the AFP-positive population in the presence of HGF and EGF. During culture on the human LN111-coated dish, the morphology of the hESC-derived HBCs gradually changed into that of human hepatoblasts (Figure S1E) (Schmelzer et al., 2007). Therefore, the characteristics of hESC-derived HBCs might be changed by culturing on a human LN111-coated dish (details of the characterization of the hESC-derived HBCs are described in Figure 3). After culturing on a human LN111-coated

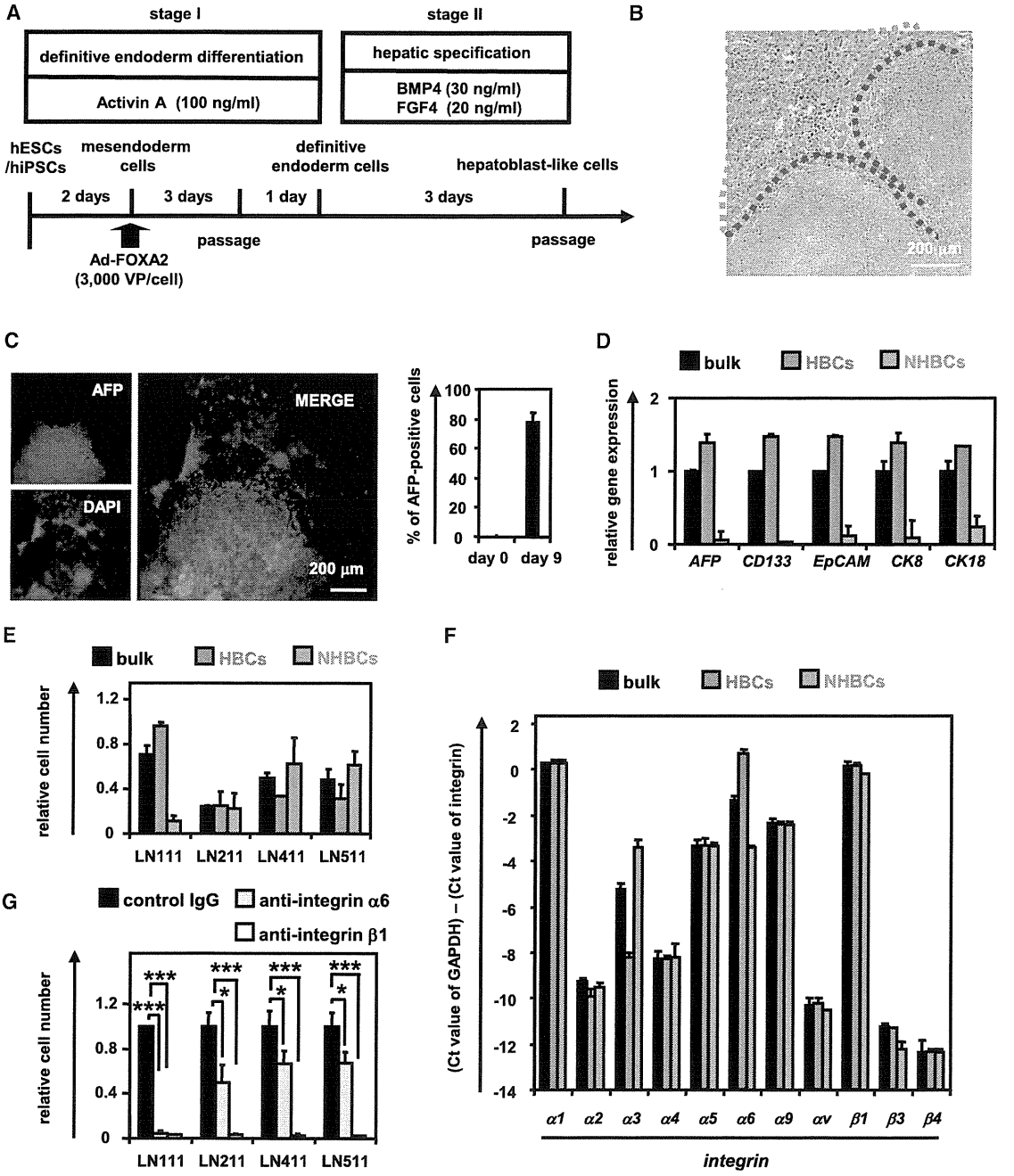

Figure 1. The Human ESC-Derived HBCs Selectively Attached to a Human LN111-Coated Dish via Integrin α6 and β1

(A) The procedure for the differentiation of hESCs (H9) into hepatoblast-like cells (HBCs) is presented schematically. Details are described in the Experimental Procedures.

(B) Phase-contrast micrographs of the hESC-derived HBCs (red) and non-HBCs (NHBCs) (green) are shown.

(C) The hESC-derived cells (day 9) were subjected to immunostaining with anti-AFP (red) antibodies. The percentage of AFP-positive cells was examined on day 0 or 9 by using FACS analysis. Data represent the mean ± SD from ten independent experiments. Cells on "day 0" and "day 9" were compared using Student's t test ($p < 0.01$).

(D) On day 9, the hESC-derived HBCs and NHBCs were manually picked, and the gene expression levels of *AFP* and pan-hepatoblast markers (*CD133*, *EpCAM*, *CK8*, and *CK18*) were measured by real-time RT-PCR. The gene expression levels of *AFP* and pan-hepatoblast markers in the hESC-derived cells (day 9; bulk) were taken as 1.0. Data represent the mean ± SD from four independent experiments. The gene expression levels in the HBCs were significantly different among the three groups (bulk, HBCs, and NHBCs) based on analysis with one-way ANOVA followed by Bonferroni post hoc tests ($p < 0.05$).

(legend continued on next page)

dish for a week, almost all of the cells were still AFP positive (Figures 2C and 2D). To characterize the cells cultured on various types of human laminins for 7 days, the gene expression levels of *AFP* and pan-hepatoblast (*CD133*, *CK8*, *CK18*, and *EpCAM*) markers were examined on day 16 (Figure 2E). The gene expression levels of *AFP* and pan-hepatoblast markers in the hESC-derived HBCs P1 (HBCs passaged once) did not change as compared with those of the hESC-derived HBCs (day 9; HBC P0) (the definitions of HBC P0, P1, P10, and clone in the present study are shown in Figure S3). The gene expression levels of mature hepatocyte and cholangiocyte markers in the hESC-derived HBC P1 did not change as compared with those of the hESC-derived HBC P0 (day 9) (Figure S1F). These results suggest that the characteristics of the hESC-derived HBC P1 are similar to those of the hESC-derived HBC P0, although their morphologies are quite different from each other. Interestingly, the gene expression levels of mature cholangiocyte markers in the cells cultured on human LN411- or 511-coated dishes were upregulated as compared with those of the hESC-derived HBC P0 (day 9) (Figure S1F), suggesting that human LN411 and 511 might promote biliary differentiation. Importantly, both hESC-derived HBCs and hiPSC-derived HBCs could extensively proliferate on a human LN111-coated dish for more than 15 passages (Figure 2F) in the presence of HGF and EGF. Doubling times of hESC (H9)-derived HBCs and hiPSC (Dotcom)-derived HBCs were approximately 78 and 67 hr, respectively. Almost all of the populations cultured on a human LN111-coated dish were AFP positive (Figure 2G). Taken together, these results suggested that the hPSC-derived HBCs would proliferate and be maintained on a human LN111-coated dish.

Characterization of the hESC-Derived HBCs

To characterize the hESC-derived HBCs, the gene expression profiles in the hESC-derived purified HBCs (HBC P0), short-term cultured HBCs (HBCs passaged once [HBC P1]), and long-term cultured HBC (HBCs passaged ten times [HBC P10]) were examined. The hESC-derived HBCs were AFP positive (Figure 3A). Although the hESC-derived HBC P0 were negative for ALB, CK7, and CK19, the hESC-derived HBC P1 and P10 were positive for these genes (Figure 3A). Both integrin α6 and β1 (receptors of LN111) were strongly expressed in the hESC-derived HBC P0, P1, and P10 (Figure 3B). The gene expression levels of human hepatic stem cell markers (*N-CAM* and *Claudin 3* [Schmelzer et al., 2007]; these are not expressed in human hepatoblasts) in the hESC-derived HBC P0 were higher than those of the hESC-derived HBC P1 and P10 (Figure 3C). However, the gene expression level of *CK19* in the hESC-derived HBC P0 was lower than that of the hESC-derived HBC P1 and P10. The gene expression levels of pan-hepatoblast markers in the hESC-derived HBC P0 were similar to those of the hESC-derived HBC P1 and P10 (Figure 3D). The gene expression levels of human hepatoblast markers (*ALB*, *CYP3A7*, and *I-CAM* (Schmelzer et al., 2007), none of which were expressed in human hepatic stem cells) in the hESC-derived HBC P1 and P10 were higher than those of the hESC-derived HBC P0 (Figure 3E). However, the AFP expression level in the hESC-derived HBC P0 was similar to that of the hESC-derived HBC P1 and P10. Because the gene expression levels of mature hepatocyte and cholangiocyte markers in the hESC-derived HBC P1 and P10 were not increased as compared with those in the hESC-derived HBC P0 (Figure 3F), the hESC-derived HBC P1 and P10 were not segregated into either of the hepatic and biliary lineages. We also examined the gene expression levels of hepatoblast markers, which have been reported only in mice and not in humans (Figure 3G). The characteristics of the hPSC-derived HBCs are summarized in Figure S3. In addition, hESC-derived HBC P0 and HBC P10 showed normal karyotypes (Figure S2A). Therefore, the genetic stability of the HBCs was confirmed throughout the maintenance period. Taken together, these results suggest that the hESC-derived HBC P0 resemble human hepatic stem cells and the hESC-derived HBC P1 and P10 resemble human hepatoblasts, although some gene expression patterns in the hESC-derived HBCs differ from those in human hepatic stem cells and human hepatoblasts, respectively.

(E) The hESC-derived cells (day 9; bulk), HBCs, and NHBCs were plated onto human LN111-, 211-, 411-, or 511-coated dishes, and the attached cells were counted at 60 min after plating. The cell number that was initially plated was taken as 1.0. Data represent the mean ± SD from four independent experiments. The number of attached HBCs on LN111-coated dishes were significantly different among three groups (bulk, HBCs, and NHBCs) based on analysis with one-way ANOVA followed by Bonferroni post hoc tests ($p < 0.05$).

(F) The gene expression levels of the indicated integrins were measured in the hESC-derived cells (day 9; bulk), HBCs, and NHBCs by real-time RT-PCR. Data represent the mean ± SD from four independent experiments. The gene expression levels of *integrin α3* and *α6* in the HBCs were significantly different among three groups (bulk, HBCs, and NHBCs) based on analysis with one-way ANOVA followed by Bonferroni post hoc tests ($p < 0.05$).

(G) The adhesion of the hESC-derived HBCs to human LN111-, 211-, 411-, or 511-coated dishes was examined by using the indicated integrin antibodies. IgG antibodies were used as a control for uninhibited cell adhesion. The number of attached cells was estimated at 60 min after plating. The cell number in the control IgG-treated group was taken as 1.0. Data represent the mean ± SD from three independent experiments. "Control IgG" and "anti-integrin α6 or integrin β1" were compared using Student's t test. *$p < 0.05$; ***$p < 0.001$. See also Figure S1 and Tables S2–S5.

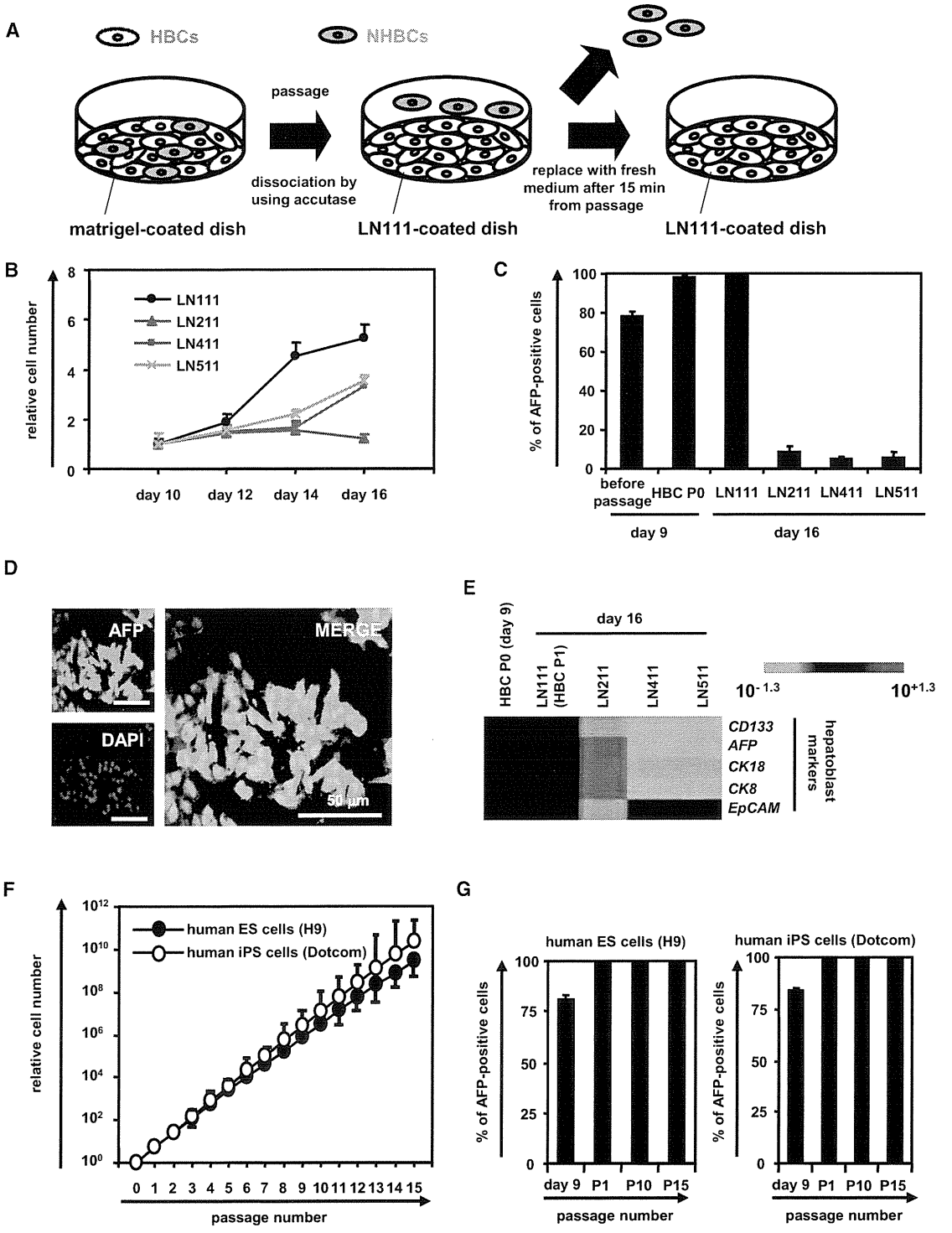

Figure 2. The hESC-Derived HBCs Could Be Proliferated and Maintained on a Human LN111-Coated Dish

(A) The hESC (H9)-derived cells (day 9) were plated onto a human LN111-coated dish. At 15 min after plating, the unattached cells were removed.

(B) The hESC (H9)-derived cells (day 9) were plated onto a human LN111, 211, 411, or 511-coated dish, and then the cell number were counted on days 10, 12, 14, and 16. The cell number on day 10 was taken as 1.0. Data represent the mean ± SD from three independent experiments. "LN111" was significantly different among four groups (LN111, 211, 411, and 511) on day 14 and 16 based on analysis with one-way ANOVA followed by Bonferroni post hoc tests ($p < 0.05$).

(legend continued on next page)

In order to examine whether the hESC-derived HBC P0 have the potential to proliferate clonally on various types of human laminins, single HBCs were plated on separate wells of a human LN111-coated 96-well plate at a low density (one cell per one well) (Table S1). Single cells that attached to the human LN111-coated dish were AFP positive and HNF4α positive (Figure S2B). At 7 days after plating, the hESC-derived HBC colonies (albumin [ALB]- and cytokeratin 7 [CK7] double positive) (a representative colony is shown in Figure S2C) were efficiently generated from the hESC-derived HBC P0 on a LN111-coated dish. Taken together, these results showed that the hESC-derived HBCs could be generated from both the hESC-derived HBC P0 population and the single hESC-derived HBC P0.

The hPSC-Derived HBCs Could Differentiate into Both Hepatic and Biliary Lineages In Vitro

To examine whether the hESC-derived HBCs have the potential to differentiate into both hepatic and biliary lineages, first, these cells were differentiated into hepatocyte-like cells as described in Figure 4A. After 2 weeks of hepatic differentiation, almost all of the cells were polygonal in shape (Figure 4B) and were CYP3A4, αAT, and ALB positive (Figure 4C). The gene expression levels of mature hepatocyte markers in the HBC P0-, HBC P10-, or HBC clone-derived hepatocyte-like cells were higher than those in the cells that had not undergone hepatic differentiation (Figure 4D), although the gene expression levels of mature cholangiocyte markers in these cells did not change (Figure 4E). The ASGR1-positive cells in the HBC P0-, HBC P10-, and HBC clone-derived population accounted for approximately 60%, 90%, and 90% of the total, respectively (Figure 4F). The HBC P0-, HBC P10-, or HBC clone-derived hepatocyte-like cells had the ability to produce ALB (Figure 4G, left) and urea (Figure 4G, right). Next, the hESC-derived HBCs were differentiated into cholangiocyte-like cells as described in Figure 4H. After 2 weeks of biliary differentiation, tubular structures (Figure 4I) that were CK7 positive (Figure 4J) were observed. Although the gene expression levels of mature hepatocyte markers (Figure 4K) in the HBC P0-, HBC P10-, or HBC clone-derived cholangiocyte-like cells did not change, the gene expression levels of mature cholangiocyte markers (Figure 4L) in these cells were higher than those in the cells that had not undergone differentiation. Similar results were obtained by using another hESC line (H1) and hiPSC line (Dotcom) (Figure S4). Moreover, HBC-derived hepatocyte-like cells exhibited CYP metabolism capacity (Figure S5A) and a functional urea cycle that could response to ammonia (Figure S5B) and were considered to have potential to be applied in the prediction of drug-induced hepatotoxicity (Figure S5C). Taken together, these results indicated that the hPSC-derived HBCs have the ability to differentiate into both hepatic and biliary lineages in vitro.

In Vivo Cell Transplantation Assays of the hPSC-Derived HBCs

To examine whether the hESC-derived HBCs could be used for hepatocyte transplantation, these cells were transplanted into CCl_4-treated immunodeficient mice as shown in Figure 5A. The hepatocyte functionality of the hESC-derived HBC P0 or HBC P10 was assessed by measuring secreted human ALB levels in the recipient mice (Figure 5B). Although human ALB was detected in the mice that were transplanted with the hESC-derived HBC P0 or HBC P10, it was not detected in the mice that were not transplanted with these cells. The ALB-positive cells were observed in mice transplanted with the hESC-derived HBC P0 or HBC P10 (Figure 5C). Most of the ALB-positive cells in mice transplanted with the hESC-derived HBC P10 were AFP negative (Figure 5D), indicating that transplanted hESC-derived HBCs were differentiated into mature hepatocyte-like cells (some of them were binuclear [Figure 5E, white arrows]). These results demonstrated that hESC-derived HBCs have the potential to be applied for hepatocyte transplantation.

(C) The hESC-derived cells (day 9) were plated onto a human LN111, 211, 411, or 511-coated dish. The percentage of AFP-positive cells was examined by using FACS analysis on day 9 (before passage and after passage [HBC P0]) or day 16. Data represent the mean ± SD from three independent experiments.
(D) The hESC-derived cells cultured on a human LN111-coated dish for 7 days were subjected to immunostaining with anti-AFP (green) antibodies.
(E) The hESC-derived cells (day 9) were plated onto human LN111, 211, 411, or 511-coated dishes. The gene expression levels of *AFP* and pan-hepatoblast markers (*CD133*, *EpCAM*, *CK8*, and, *CK18*) were measured by real-time RT-PCR on day 16. The gene expression levels in the hESC-derived HBCs (the LN111-attached cells were collected at 15 min after plating) were taken as 1.0.
(F) The HBCs derived from hESCs (H9) or hiPSCs (Dotcom) were cultured and cell growth was analyzed by obtaining a cell count at each passage. Data represent the mean ± SD from three independent experiments.
(G) The percentage of AFP-positive cells was examined by using FACS analysis on day 9 (before passage), P1 (HBCs passaged once), P10 (HBCs passaged ten times), and P15 (HBCs passaged 15 times). Data represent the mean ± SD from seven independent experiments.
See also Tables S2 and S3.

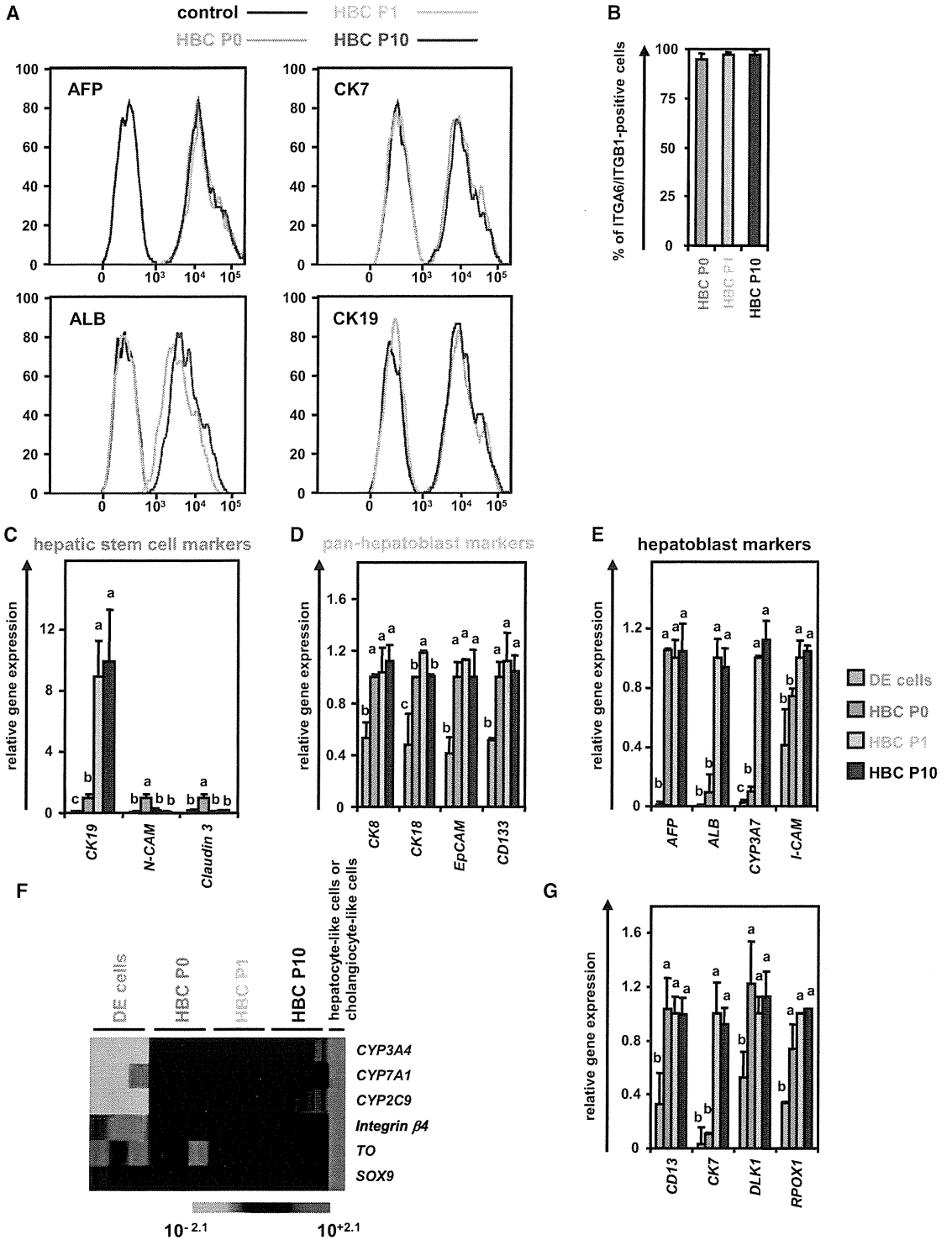

Figure 3. The hESC-Derived HBCs Were Characterized

(A and B) The hESCs (H9) were differentiated according to Figure 1A and then passaged onto a human LN111-coated dish. The attached cells (hESC-derived HBCs [HBC P0]) were collected at 15 min after plating. The percentage of AFP-positive, ALB-positive, CK7-positive, CK19-positive (A), and integrin α6- and integrin β1-double positive (B) cells in the hESC-derived HBC P0, HBC P1 (HBCs passaged once), and HBC P10 (HBCs passaged ten times) populations was estimated by using FACS analysis. Data represent the mean ± SD from seven independent experiments.

(legend continued on next page)

DISCUSSION

The main purpose of this study was to establish and characterize expandable HBCs from hPSCs. First, we identified that human LN111 could support self-renewal and proliferation of hPSC-derived HBCs in the presence of HGF and EGF. Second, we showed that the hPSC-derived HBCs have the potential to segregate into both hepatic and biliary lineages, and to integrate into the mouse liver parenchyma.

We have demonstrated that the hPSC-derived HBCs could be maintained on a human LN111-coated dish in an integrin α6- and β1-dependent manner (Figure 1). It is known that undifferentiated hPSCs could be maintained on a human LN511-coated dish but not on a human LN111-coated dish (Rodin et al., 2010). This might suggest that human LN111 has the potential not only to selectively maintain HBCs, but also to eliminate residual undifferentiated cells. Our hepatoblast-like cells could efficiently proliferate for more than 3 months on a human LN111-coated dish (Figure 2). In the human liver development (during 5–10 weeks gestation), laminin is observed in both the perisinusoidal space and portal tracts (Couvelard et al., 1998). The expression of laminin is localized around the periportal biliary trees during the later stage of liver development (Couvelard et al., 1998). Hepatic stem cells reside around the hepatic portal area (Clément et al., 1988). It is also known that laminin is accumulated around oval cells although laminin is not expressed around quiescent mature hepatocytes (Paku et al., 2001). These facts suggest that laminin plays an important role in the maintenance and proliferation of hepatoblasts.

The hPSC-derived HBC P10 and clone were positive for hepatoblast markers (AFP, ALB, CYP3A7, and I-CAM), but negative for hepatic stem cell markers (N-CAM and Claudin 3) (Figure 3) (Schmelzer et al., 2007). Although the hPSC-derived HBCs were able to expand on human LN111-coated dish, Schmelzer et al. showed that human hepatoblasts do not proliferate under a monolayer culture condition, but human hepatic stem cells could self-replicate for more than 6 months (Schmelzer et al., 2007). Although further investigations of the hepatoblast characteristics in the hPSC-derived HBCs will be needed in the future, the results in the present study suggest that the characteristics of hPSC-derived HBCs expanded on human LN111-coated dishes were similar to those in human hepatoblasts isolated from the human liver (Schmelzer et al., 2007; Zhang et al., 2008).

The hPSC-derived HBCs had the ability to integrate into the mouse liver parenchyma (Figure 5), in the manner of human hepatic stem cells or hepatoblasts (Schmelzer et al., 2007). The human ALB serum levels (approximately 20–70 ng/ml) in mice transplanted with the hESC-derived HBC P0 or HBC P10 were comparable to those in the previous paper in which the hESC-derived definitive endoderm cells, hepatoblasts, and hepatocyte-like cells were transplanted into mice (Liu et al., 2011), but were lower than those of human liver chimeric mice (Tateno et al., 2004). Human ALB serum levels would increase if more suitable host mice, such as urokinase plasminogen activator-SCID mice were used (Tateno et al., 2004).

In this study, we have developed a technology for the maintenance and proliferation of hPSC-derived HBCs by using human LN111. To transplant these cells for purposes of regenerative medicine, a xeno-free culture condition for hPSC-derived HBCs must be developed in the future. It is hoped that the hPSC-derived HBCs and their derivatives will be helpful in various medical applications, such as drug screening and regenerative medicine.

EXPERIMENTAL PROCEDURES

hESC and hiPSC Culture

The hESC lines (H1 [WA01] and H9 [WA09] [WiCell Research Institute]) and the hiPSC line, Dotcom (JCRB number: JCRB1327) (Makino et al., 2009; Nagata et al., 2009), were maintained on a feeder layer of mitomycin-C-treated mouse embryonic fibroblasts (Millipore) with ReproStem medium (ReproCELL) supplemented with 5 and 10 ng/ml fibroblast growth factor 2 (FGF2) (Katayama Kagaku Kogyo), respectively. H1 and H9 were used following the Guidelines for Derivation and Utilization of Human Embryonic Stem Cells of the Ministry of Education, Culture, Sports, Science and Technology of Japan, and, furthermore, the study was approved by an independent ethics committee.

In Vitro Hepatoblast Differentiation

The differentiation protocol for the induction of definitive endoderm cells and hepatoblasts was based on our previous report with some modifications (Inamura et al., 2011; Takayama et al., 2012a, 2012b, 2013). In mesendoderm differentiation, hESCs/iPSCs were

(C–F) The gene expression levels of hepatic stem cell markers (C), pan-hepatoblast markers (D), hepatoblast markers (E), and mature hepatocyte (*CYP3A4*, *7A1*, *2C9*, and *TO*) or cholangiocyte markers (*integrin β4* and *SOX9*) (F) were measured in the definitive endoderm cells, HBC P0, HBC P1, or HBC P10 by real-time RT-PCR.

(G) The gene expression levels of *CD13*, *CK7*, *DLK1*, and *PROX1* were measured in the hESC-derived definitive endoderm cells, HBC P0, HBC P1, or HBC P10 by real-time RT-PCR. Data represent the mean ± SD from three independent experiments. Statistical significance was evaluated by ANOVA followed by Bonferroni post hoc tests to compare four groups (DE cells, HBC P0, HBC P1, and HBC P10). Groups that do not share the same letter are significantly different from each other ($p < 0.05$). DE, definitive endoderm cells.

See also Figures S2 and S3 and Tables S2–S4.

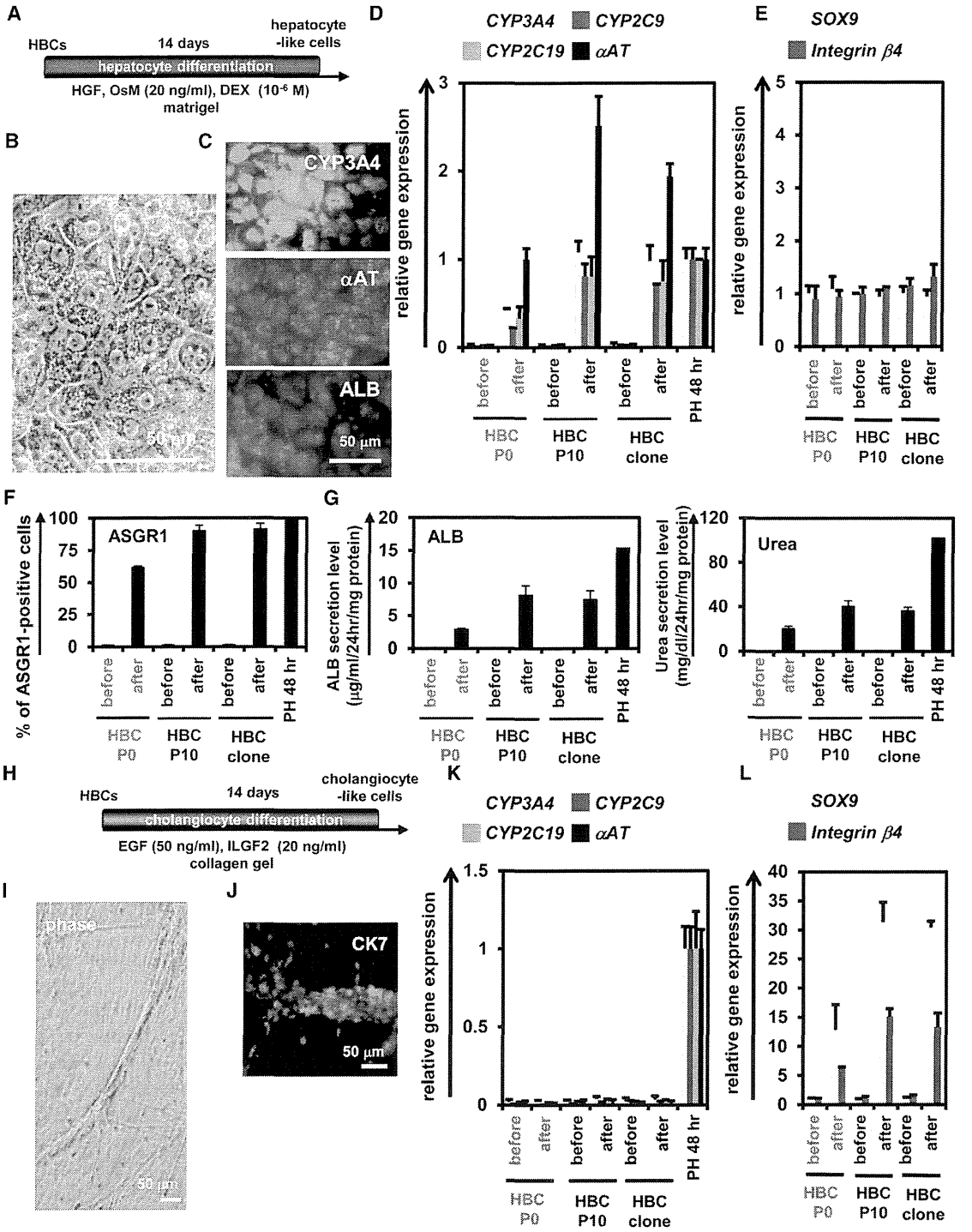

Figure 4. The hESC-Derived HBCs Could Differentiate into Both Hepatic and Biliary Lineages

(A) The procedure for differentiation of the hESC (H9)-derived HBC P0, HBC P10, or HBC clone into the hepatocyte-like cells is presented schematically. Details are described in Experimental Procedures.

(B) Phase-contrast micrographs of the HBC P10-derived hepatocyte-like cells are shown.

(C) The HBC P10-derived hepatocyte-like cells were subjected to immunostaining with anti-CYP3A4 (green), anti-αAT (red), and anti-ALB (red) antibodies.

(D and E) The gene expression levels of hepatocyte (D) or cholangiocyte (E) markers in HBC P0-, HBC P10-, or HBC clone-derived hepatocyte-like cells were measured by real-time RT-PCR after 14 days of hepatocyte differentiation. In (D), the gene expression levels in

152 (legend continued on next page)

cultured for 2 days on Matrigel (BD Biosciences) in differentiation hESF-DIF medium that contains 100 ng/ml Activin A (R&D Systems) (hESF-DIF medium was purchased from Cell Science & Technology Institute; differentiation hESF-DIF medium was supplemented with 10 μg/ml human recombinant insulin, 5 μg/ml human apotransferrin, 10 μM 2-mercaptoethanol, 10 μM ethanolamine, 10 μM sodium selenite, and 0.5 mg/ml bovine fatty acid free serum albumin [all from Sigma]). To generate definitive endoderm cells, the mesendoderm cells (day 2) were transduced with 3,000 vector particle (VP)/cell of FOXA2-expressing adenovirus vectors (Ad-FOXA2) for 1.5 hr and cultured until day 6 on Matrigel in differentiation hESF-DIF medium supplemented with 100 ng/ml Activin A. For induction of hepatoblasts, the definitive endoderm cells were cultured for 3 days on a Matrigel in differentiation hESF-DIF medium supplemented with 30 ng/ml bone morphogenetic protein 4 (BMP4) (R&D Systems) and 20 ng/ml FGF4 (R&D Systems).

Establishment and Maintenance of the hPSC-Derived HBCs

The hPSC-derived HBCs were first purified from the hPSC-derived cells (day 9) by selecting attached cells on a human recombinant LN111 (BioLamina)-coated dish at 15 min after plating. The hPSC-derived HBCs were cultured on a human LN111-coated dish (2.0×10^4 cells/cm^2) in maintenance DMEM/F12 medium (DMEM/F12 medium [Invitrogen] was supplemented with 10% FBS, 1 × insulin/transferrin/selenium, 10 mM nicotinamide, 10^{-7} M dexamethasone (DEX) (Sigma), 20 mM HEPES, 25 mM $NaHCO_3$, 2 mM L-glutamine, penicillin/streptomycin, 40 ng/ml hepatocyte growth factor [HGF] [R&D Systems] and 20 ng/ml epidermal growth factors [EGF] [R&D Systems]). The medium was refreshed every day. The hPSC-derived HBCs were dissociated with Accutase (Millipore) into single cells and subcultured every 6 or 7 days.

Establishment and Maintenance of a Single hPSC-Derived HBC

For single-cell culture, the single HBC was plated to separate well of human LN111-coated 96-well plate in maintenance DMEM/F12 medium supplemented with 25 μM Y-27632 (ROCK inhibitor) (Millipore), and then colonies derived from a single cell were manually picked up and cultured as well as HBCs (these cells were designated the HBC clone).

In Vitro Hepatocyte and Cholangiocyte Differentiation

To induce hepatocyte differentiation, the hPSC-derived HBC P0, HBC P10, and HBC clone were cultured for 14 days on a Matrigel-coated dish (7.5×10^4 cells/cm^2) in HCM (Lonza) supplemented with 20 ng/ml HGF, 20 ng/ml Oncostatin M (OsM) (R&D Systems), and 10^{-6} M DEX. To induce cholangiocyte differentiation, the hPSC-derived HBC P0, HBC P10, and HBC clone were cultured in collagen gel for 14 days. To establish collagen gel plates, 500 μl collagen gel solution (consisting of 400 μl type I-A Collagen (Nitta gelatin), 50 μl 10 × DMEM, and 50 μl of 200 mM HEPES buffer containing 2.2% $NaHCO_3$ and 0.05 M NaOH) was added to each well, and then the plates were incubated at 37°C for 30 min. The hPSC-derived HBC P0, HBC P10, and HBC clone (5×10^4 cells) were resuspended in 500 μl differentiation DMEM/F12 medium (differentiation DMEM/F12 medium was supplemented with 20 mM HEPES, 2 mM L-glutamine, 100 ng/ml EGF, and 40 ng/ml insulin-like growth factor 2 [ILGF2]), and then mixed with 500 μl of the collagen gel solution and plated onto the basal layer of collagen. After 30 min, 2 ml of differentiation DMEM/F12 medium was added to the well.

Ad Vectors

Ad vectors were constructed by an improved in vitro ligation method. The human EF-1α promoter-driven FOXA2-expressing Ad vectors (Ad-FOXA2) were constructed previously (Takayama et al., 2012b). All of Ad vectors contain a stretch of lysine residue (K7) peptides in the C-terminal region of the fiber knob for more efficient transduction of hESCs, hiPSCs, mesendoderm cells, and definitive endoderm cells, in which transfection efficiency was almost 100%, and purified as described previously (Inamura

PH 48 hr were taken as 1.0. In (E), the gene expression levels in HBC P10 (before differentiation) were taken as 1.0. Data represent the mean ± SD from three independent experiments. Student's t test indicated that gene expression levels of the hepatocyte markers in "after" were significantly higher than those in "before" ($p < 0.01$).

(F) The efficiency of hepatocyte differentiation was measured by estimating the percentage of ASGR1-positive cells using FACS analysis.

(G) The amounts of ALB (left) and urea (right) secretion were examined. Data represent the mean ± SD from three independent experiments. Student's t test indicated that the percentage of ASGR1-positive cells, the ALB secretion level, and urea secretion level in "after" were significantly higher than those in "before" ($p < 0.01$).

(H) The procedure for the differentiation of the hESC-derived HBC P0, HBC P10, or HBC clone into cholangiocyte-like cells is presented schematically. Details are described in Experimental Procedures.

(I) Phase-contrast micrographs of the HBC P10-derived cholangiocyte-like cells are shown.

(J) The HBC P10-derived cholangiocyte-like cells were subjected to immunostaining with anti-CK7 (red) antibodies.

(K and L) The gene expression levels of hepatocyte (K) or cholangiocyte (L) markers in the HBC P0-, HBC P10-, or HBC clone-derived cholangiocyte-like cells were measured by real-time RT-PCR after 14 days of cholangiocyte differentiation. In (K), the gene expression levels in PH 48 hr were taken as 1.0. In (L), the gene expression levels in HBC P10 (before cholangiocyte differentiation) were taken as 1.0. Data represent the mean ± SD from three independent experiments. Student's t test indicated that the gene expression levels of cholangiocyte markers in "after" were significantly higher than those in "before" ($p < 0.01$). "Before" indicates the HBCs before hepatocyte or cholangiocyte differentiation; "After" indicates the HBCs after hepatocyte or cholangiocyte differentiation.

See also Figures S4 and S5 and Tables S1–S4.